Construction and Characterization of [1,6-Di(*N*-carbazolyl)-2,4-hexadiyne] Diacetylene Polymer Bicrystals

Jun Liao† and David C. Martin*

Department of Materials Science and Engineering and the Macromolecular Science and Engineering Center, 2022 H. H. Dow Building, The University of Michigan, Ann Arbor, Michigan 48109-2136

Received June 5, 1995; Revised Manuscript Received August 29, 1995⊗

ABSTRACT: We have developed schemes to construct and characterize the microstructure and macroscopic properties of individual grain boundary defects in extended-chain, conjugated polymers. Our approach has been to take [1,6-di(*N*-carbazolyl)-2,4-hexadiyne] (DCHD) diacetylene monomer crystals and introduce a single defect under specified boundary conditions. Two monomer seed crystals are cut from a precursor single crystal and then brought into close proximity with one another. Monomer bicrystals are created by a recrystallization step involving slow evaporation of a DCHD solution. The monomer bicrystals are then converted into polymer bicrystals through thermal energy or by exposure to high-energy radiation. We have found that the ability to retain a cohesive interface between the crystals after the solid-state reaction is a sensitive function of their relative misorientation and the method of polymerization. In general, small-angle grain boundaries remain intact, while large-angle grain boundaries are broken after polymerization. The geometrical conditions required to obtain a coherent interface are more stringent for radiation than thermal polymerization. The macroscopic properties of the polymer bicrystals are particularly sensitive to the geometry of the interface. The efficiency of photoconductive charge carrier transport across the grain boundary decreases systematically with increasing misorientation. The mechanical strength of the polymer bicrystals also decreases with increasing misorientation between crystals, with the fracture localized to the engineered interface. Our results are consistent with decreasing covalent bond connectivity of the polymer chains across the interface with increasing misorientation angle.

INTRODUCTION

Ordered, conjugated polymers are of interest for a number of photonic and electronic applications including waveguides, frequency doublers, light-emitting diodes, thin-film transistors, and gas sensors.[1] In order to realize the full potential of these polymer-based devices, it will be necessary to develop schemes to precisely and reproducibly control microstructure and macroscopic properties through novel molecular designs and processing.

The ability to tailor the properties of materials in the solid state requires an intimate understanding of the variations in microstructure near defects. In metallic and organic solids, defects such as grain boundaries play an important role in modifying macroscopic properties. In order to understand the influence of a particular defect on the properties of materials, it has proven useful to isolate single defects by creating bicrystals with a single, predominant interface. In this way the geometry of the grain boundary defect can be controlled and its influence on properties determined unambiguously. For example, in superconducting copper oxides it has been found that the critical current J_c decreases with increasing twist or tilt misorientation between crystals.[2] In certain cases, it has been possible to design grain boundaries which have useful properties that can be exploited. For example, high-T_c superconductor devices have been fabricated in which the defects form a controlled, weak-link junction.[3,4]

In crystalline polymers, it would be valuable to establish a similar depth of understanding about the relationship between defect structure and macroscopic properties. Conventional semicrystalline polymers typically have small, lamellar crystallites (10−20 nm). This implies a large defect density in the solid state. However, the development of solid-state and thin-film polymerization schemes has facilitated the synthesis of highly ordered polymer systems. These materials make it possible to investigate the structure and properties of organic solids near defects.

The purpose of this paper is to present a scheme for introducing specific grain boundary defects into ordered polymers so that their influence on macroscopic properties can be isolated and studied in detail. Our goal has been to establish a framework for examining the influence of systematic variations in polymer morphology on macroscopic properties. We also suspect that similar procedures could be adapted to investigate defect-mediated phenomena in organic molecular crystals. Our experimental protocol involves (a) construction of diacetylene monomer bicrystals with controlled grain boundary geometries, (b) transformation of these monomer bicrystals into polymer bicrystals *via* solid-state polymerization, and (c) characterization of the macroscopic properties and microstructure of the bicrystals as a function of grain boundary geometry.

BACKGROUND

Disubstituted diacetylene monomers are capable of producing highly ordered, extended conjugated molecules by solid-state polymerization.[5] Diacetylene polymers can be synthesized by heat, light, or high-energy radiation in the solid state from the precursor monomer without loss of crystallinity. Large diacetylene monomer single crystals can be grown from solution. We thus should be able to construct diacetylene monomer bicrystals and then transform them into polymer bicrys-

† Current address: Mt. Vernon Technology, GE Plastics, 1 Lexan Lane, Mt. Vernon, IN 47620-9364.

⊗ Abstract published in *Advance ACS Abstracts,* December 1, 1995.

0024-9297/96/2229-0568$12.00/0

tals through a solid-state polymerization without loss of crystallinity.

The solid-state diacetylene polymerization is a topochemical process by which the monomer crystals react to yield nearly perfect polymer crystals under the constraint of the crystal lattice. Using the principles of least motion, Baughman proposed that the reaction pathway of diacetylene monomers would be one in which the smallest mean square displacement of the atoms would take place.[6] The optimum conditions for the phase transformation are that the packing angle γ between the polymer chain and the center of mass should be less than 45° and the relative lattice contraction $(d_1 - d_2)/d_2$ during the phase transformation should not exceed 0.1. Under these geometric packing conditions, diacetylene monomer molecules rotate about their center of mass but keep the crystal lattice intact. The diacetylene phase transformation has been examined by variety of techniques including polarized optical microscopy,[7] X-ray diffraction,[7,8] X-ray topography,[9−12] and electron diffraction.[13]

There have been a limited number of observations of grain boundary defects in diacetylene polymers. By mechanically deforming diacetylene single crystals, Young et al. introduced twins and observed the twin boundary structures using TEM.[14−17] Day and Lando deposited polymerizable Langmuir−Blodgett monolayers of diacetylenes onto glass slides and found that they would often crack at the boundaries between domains of locally oriented polymer.[18] Their observations suggested that large-angle grain boundaries between domains do not facilitate the polymerization of diacetylenes. However, the structure and properties of these grain boundaries and twin boundaries remained to be studied in depth.

Martin and Thomas[19] discussed the structure, energetics, and mobility of grain boundaries in extended-chain polymers. This work was inspired by HRTEM studies of the rigid-rod polymers poly(*p*-phenylenebenzobisthiazole) (PBZT) and poly(*p*-phenylene benzobisoxazole) (PBZO).[20] These studies qualitatively established a fundamental basis for analyzing the energetics and geometry of grain boundary defects. Gido and Thomas examined grain boundary morphology and energetics in microphase-separated diblock copolymers.[21−23] However, the ability to unambiguously establish the relationship between grain boundary structure and macroscopic properties has remained elusive, because it has been difficult to isolate a single, predominant defect to study in detail.

Diacetylene polymers exhibit a fully conjugated and planar backbone in the crystalline state. Many diacetylenes possess attractive mechanical, electrical and optical properties. For example, the mechanical strength of diacetylene needle crystals can be as high as 2 GPa.[24−26] Their nonlinear optical properties ($\chi^{(3)} = 1.0 \times 10^{-10}$ esu at 1.064 μm, and 6.0×10^{-10} esu at 1.907 μm)[27] have generated interest in their potential use for optoelectronic devices.[28−31]

The 1,6-di(*N*-carbazolyl)-2,4-hexadiyne (DCHD) diacetylene was first synthesized by Yee and Chance:[32]

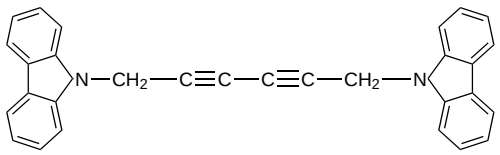

1,6-di(*N*-carbazoyl)-2,4-hexadiyne (DCHD)

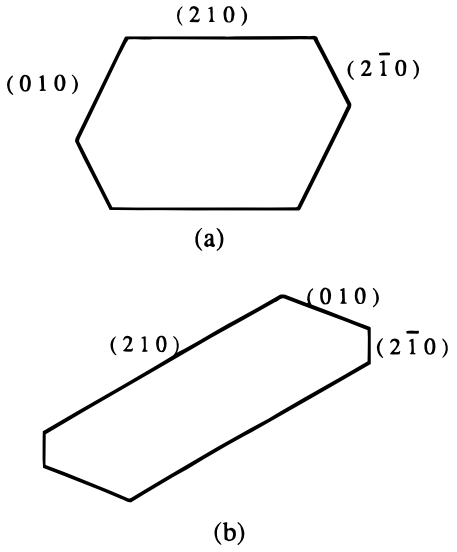

Figure 1. Schematics showing cross sections of DCHD monomer crystals on the (001) faces perpendicular to the polymer chains: (a) approximately hexagonal, and (b) ribbonlike. The (2 1 0), (2 1̄ 0), and (0 1 0) crystallographic faces are indicated.

DCHD monomer and polymer crystals are both monoclinic: the monomer has a space group of $P2_1/c$ with $a = 1.760$ nm, $b = 1.360$ nm, $c = 0.455$ nm, and $\gamma = 94.0°$; [33] the polymer also has the same space group with $a = 1.739$ nm, $b = 1.289$ nm, $c = 0.490$ nm, and $\gamma = 108°$.[34]

DCHD crystals are needle-shaped, with the [0 0 1] direction oriented along the long axis of the crystal. The cross sections of the crystals perpendicular to [0 0 1] are approximately hexagonal or ribbonlike, as shown in Figure 1.[7,35] The faces of the crystals have been indexed as the (2 1 0), (2 1̄ 0), and (0 1 0) crystallographic planes. Figure 2a is the molecular projection down the [0 0 1] axis of the DCHD diacetylene monomer crystal. Figure 2b is the molecular projection on the (0 1 0) plane. Figure 3 is the molecular projection down the [0 0 1] axis of the DCHD diacetylene polymer crystal.

By measuring the mechanical strength and the transient photoconductivity of constructed diacetylene polymer bicrystals as a systematic function of bicrystal geometry, we expect to obtain insight about the ability to form covalent bonds as the local symmetry near the interface changes. Adam et al. conducted studies of the structural evolution in a discotic liquid crystal by measuring transient photoconductivity as a function of temperature.[36] Through these studies, they utilized photoconductivity as a tool to detect the influence of molecular ordering and microstructure on macroscopic properties. Our studies here are intended to reveal polymer chain connectivity across grain boundary interfaces with different misorientation angles.

The relationship between microstructure and mechanical properties of DCHD diacetylene polymer crystals has been studied by scanning electron microscopy (SEM) and transmission electron microscopy (TEM).[26,35,37] The mechanical strength decreases as the crystal diameter increases.[37,38] This was attributed to the existence of defects such as surface steps. Deformation twinning in diacetylene polymer crystals has been investigated by SEM, TEM, and optical microscopy.[39−41] In DCHD, the twins have been identified to have K_1 twinning planes of (2 1̄ 2) with the K_2 plane of rotated simple shear equal to (2 1̄ 0).[41]

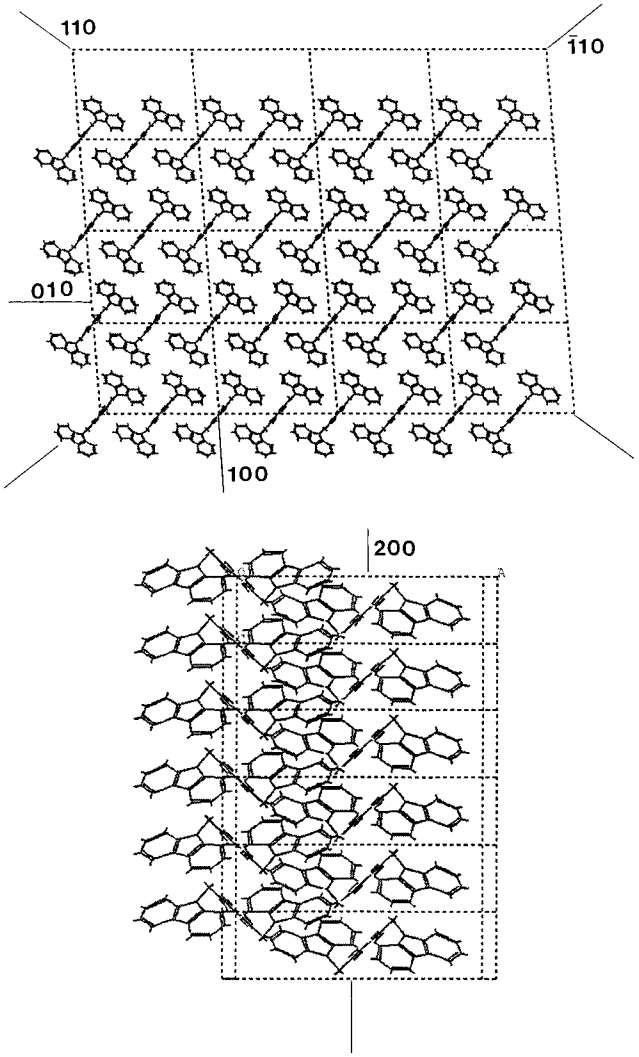

Figure 2. (a, top) Molecular projection down the [0 0 1] direction of DCHD diacetylene monomer crystals. (b, bottom) Molecular projection on the (0 1 0) plane of DCHD diacetylene monomer crystals.

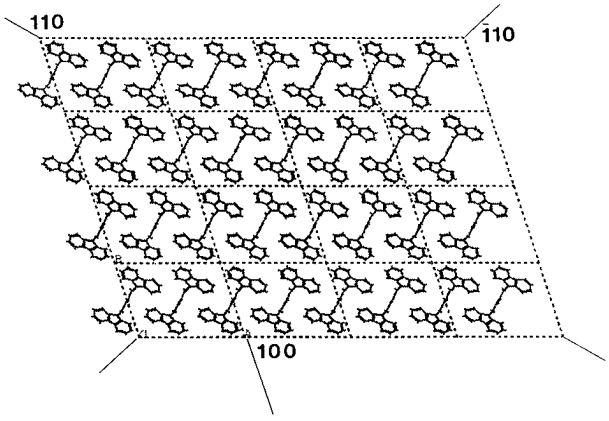

Figure 3. Molecular projection down the [0 0 1] axis, the polymer backbone of DCHD diacetylene polymer crystals.

Diacetylene polymers are quasi-one-dimensional photoconductors. The photoinduced electrical carrier mobility along the polymer chain direction has been measured to be about 5 $cm^2/V{\cdot}s$[42,43] and is 3−4 orders of magnitude higher than that perpendicular to the polymer chain direction. Diacetylene polymers have been utilized to study carrier motion along the chain in semiconductive conjugated polymer solids. Defects are recognized to be traps for carrier transport in semiconductors.[44] They should also behave as traps to carrier transport in diacetylene polymer crystals.

There have been a number of studies of the mechanisms of charge carrier transport in conjugated diacetylene polymers. Donovan and Wilson obtained a carrier velocity of 2200 m/s, essentially independent of the applied electrical field down to 1 V/cm, which gives rise to an ultrahigh low-field mobility of 2×10^5 $cm^2/V{\cdot}s$.[45] Wilson thus proposed that the carriers move as a solitary wave acoustic polaron (SWAP).[46] A SWAP is formed from the interaction of a free-band electron with the acoustic phonons. In one dimension, the lattice deforms locally around the electron to form a polaron. The SWAP has a very large effective mass and cannot move at a velocity greater than sound. The energy is dissipated by bouncing the existing ambient acoustic phonons with a Doppler shift off the SWAP. This process is weak and thus the dissipation by the SWAP is also weak. However, Fisher found that carrier velocity is dependent on the electrical field at low field but tends to be saturated at 5000 m/s at electrical fields higher than 6.5×10^4 V/cm.[43] He accordingly suggested that carrier motion along a chain may be that of the SWAP, but the observed motion is dominated by field-dependent trapping events at low fields. Based on the concept of the SWAP, he assumed the presence of "shallow" Coulomb trapping which is temperature dependent and inversely proportional to the electrical field. This model seems to explain his observations of the effect of electrical field on the intrinsic motion of carriers along the chain.

The precise relationship between charge carrier transport and defect structure of diacetylenes has not yet been established in detail. Donovan and Wilson cut the surfaces of pTS crystals periodically and revealed that charge carriers were not trapped by these cuts until they traveled about 1 mm.[47,48] It was also found that a series of lines written with an electron beam reduced carrier transport in DCHD.[49] These studies demonstrated that purposely introduced defects could limit the electrical properties of diacetylene polymers. Here, we examine the influence of well-defined grain boundary defect structures on the charge carrier transport properties of DCHD.

To measure transient photoconductivity, a modified time-of-flight technique has been used.[50,51] The charge carriers are generated by a pulsed light source and driven through the sample by an applied electric field. Any traps or recombination centers within the samples will delay the time of flight of the charge carriers or weaken the photocurrent intensity. The time-of-flight technique has proven useful to examine charge carrier drift mechanisms in photoconductors. It has also been used to study electrical transport mechanisms in diacetylene polymer single crystals.[43,45,47−49,52,53]

In our studies, the Auston gap transmission line geometry was used due to the flexibility of making micrometer-sized gaps. In an Auston gap transmission line, two electrodes are pasted or deposited on the tested surfaces. The Auston gap transmission line yields insight about the electrical transport in a thin region near the surface of the sample corresponding to the penetration depth of the UV laser ($<100\ \mu m$).[53] In our case, the gap contains a grain boundary which is covered by a mask to prevent it from laser illumination. We excite carriers on one side of the grain boundary, drive charge carriers through the grain boundary, and measure the transient photoconductivity as a function of

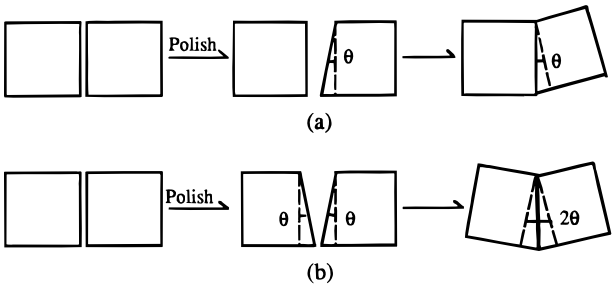

Figure 4. Schematic of the procedure for constructing (a) an asymmetric monomer tilt bicrystal and (b) a symmetric monomer tilt bicrystal. To construct an asymmetric monomer bicrystal, a DCHD diacetylene monomer single crystal is cut into two halves by sectioning perpendicular to the [0 0 1] direction. One of the cut surfaces is then polished by an angle θ. Keeping the (2 1 0) edges on the (0 0 1) cut surfaces parallel and putting the unpolished half and polished half back together, we construct an asymmetric monomer tilt bicrystal with θ degree of tilt of the [0 0 1] about the (2 1 0) edge (the [$\bar{1}$ 2 0] direction). If we polish both cut surfaces by the same angle θ, we end up with a symmetric monomer tilt bicrystal having 2θ degree of tilt of the [0 0 1].

grain boundary geometry. Both the grain boundary geometry and field strength dependence of photocurrent and carrier drift mobility have been examined.

BICRYSTAL CONSTRUCTION

Grain boundaries are the interfaces separating two joined crystals of the same kind, but rotated and/or twisted with respect to one another. A grain boundary has five degrees of freedom.[54] This involves three degrees of freedom to determine the relative orientation of the two component grains and two degrees of freedom to define the orientation and position of the boundary surface. Martin and Thomas presented a classification scheme for describing the geometry of grain boundaries in extended-chain polymers.[19] Defining the polymer chain directions in each grain as C_1 and C_2, respectively, they proposed four categories of grain boundaries based on whether C_1 and C_2 are parallel in both grains and whether the grain boundary plane is parallel to C_1 and C_2. If C_1 and C_2 are parallel, the grain boundary is a "chain invariant" boundary, otherwise it is a "chain rotation" boundary. If the grain boundary plane is parallel to C_1 and C_2, then it is a "lateral boundary", otherwise it is an "axial boundary". Therefore, the four types of grain boundaries in polymer solids are (1) lateral chain invariant (LCI), (2) axial chain invariant (ACI), (3) lateral chain rotation (LCR), and (4) axial chain rotation (ACR) boundaries.

We confirmed the crystallographic indexing of the DCHD crystal faces with an optical goniometer.[55] After a DCHD monomer crystal is cut into two seed crystals, corresponding edges on the cut surfaces and the *c*-axis ([0 0 1]) are selected as coordinate axes for bicrystal construction. The orientation is defined by the relative rotation of these axes, ψ, ϕ, and θ. The orientation of the grain boundary plane is constrained by the cut surfaces facing each other.

The construction of DCHD diacetylene polymer bicrystals requires (1) the preparation of DCHD diacetylene monomer bicrystals and (2) the solid-state phase transformation of DCHD diacetylene monomer bicrystals into polymer bicrystals. Figure 4 is a schematic of the procedure for constructing (a) an asymmetric monomer tilt bicrystal and (b) a symmetric monomer tilt bicrystal. To construct an asymmetric monomer bicrystal, as shown in Figure 4a, a DCHD diacetylene monomer single crystal is cut into two halves by sectioning perpendicular to the *c*-axis ([0 0 1]). One of the cut surfaces is then polished by an angle θ. We take the (2 1 0) edge on the (0 0 1) cut surfaces (the [$\bar{1}$ 2 0] direction) as a reference. Thus, by keeping the (2 1 0) edges on the two cut surfaces parallel and putting the unpolished half and polished half back together, we construct an asymmetric monomer tilt bicrystal with θ degree tilting of the [0 0 1] direction about the (2 1 0) edge. Knowing that the (0 0 1) cross section is terminated by (0 1 0), (2 1 0), and (2 $\bar{1}$ 0) planes as shown in Figure 1, we select the (2 1 0) and (0 1 0) edges on the (0 0 1) face and [0 0 1] direction as coordinate axes. The relative orientation between the grains and the grain boundary plane can be described as following:

$$(0\ 1\ 0)_{\text{grain 1}} \,//\, (0\ 1\ 0)_{\text{grain 2}}$$

$$(2\ 1\ 0)_{\text{grain 1}} + \theta \,//\, (2\ 1\ 0)_{\text{grain 2}}$$

$$[0\ 0\ 1]_{\text{grain 1}} + \theta = [0\ 0\ 1]_{\text{grain 1}}$$

$(0\ 0\ 1)$—the grain boundary plane of grain 1

If we polish both cut surfaces by the same angle θ, we end up with a symmetric monomer tilt bicrystal, as shown in Figure 4b, having a 2θ degree tilting of the [0 0 1] direction about the [$\bar{1}$ 2 0] axis (the (2 1 0) edge). The relationships between the five degrees of freedom are the same as above, but there is now a 2θ angle of tilt between the [0 0 1] directions and both grains share a common grain boundary plane that makes an angle θ with (0 0 1). Due to the difficulty of obtaining the same polishing angle θ in Figure 4b, it is easier to construct an asymmetric tilt bicrystal than a symmetric one. Therefore, we focused our attention on asymmetric tilt bicrystals for simplicity. Both asymmetric and symmetric tilt grain boundaries are ACR boundaries.

Figure 5 is a schematic demonstrating that the (2 1 0) edge (the [$\bar{1}$ 2 0] direction) on the (0 0 1) cross section is taken as the rotation axis during the construction of the tilt bicrystals. After grain A rotates about the [$\bar{1}$ 2 0] axis by an angle θ, there is an angle θ tilting of the [0 0 1] direction between A and B and $(2\ 1\ 0)_A$ makes an angle θ with $(2\ 1\ 0)_B$.

Figure 6 is a schematic of the construction of a pure twist bicrystal. In this case we take one edge, e.g., the (2 1 0) edge, on one cut surface as a reference and rotate the corresponding edge on another surface about the [0 0 1] direction under an optical microscope by an angle ψ. A monomer twist bicrystal with ψ degrees of twisting about the [0 0 1] is then defined and constructed. Given that the (0 0 1) cross section is terminated by the (0 1 0) and (2 1 0) faces, the five degrees of freedom determining the relative orientation between each grain and the orientation of the grain boundary plane in this case are

$$(0\ 1\ 0)_{\text{grain 1}} + \psi = (0\ 1\ 0)_{\text{grain 2}}$$

$$(2\ 1\ 0)_{\text{grain 1}} + \psi = (2\ 1\ 0)_{\text{grain 2}}$$

$$[0\ 0\ 1]_{\text{grain 1}} \,//\, [001]_{\text{grain 2}}$$

$(0\ 0\ 1)_{\text{grain 1}} \,//\, (0\ 0\ 1)_{\text{grain 2}}$—the grain boundary plane

Since the chain directions are parallel, twist grain boundaries are ACI boundaries.

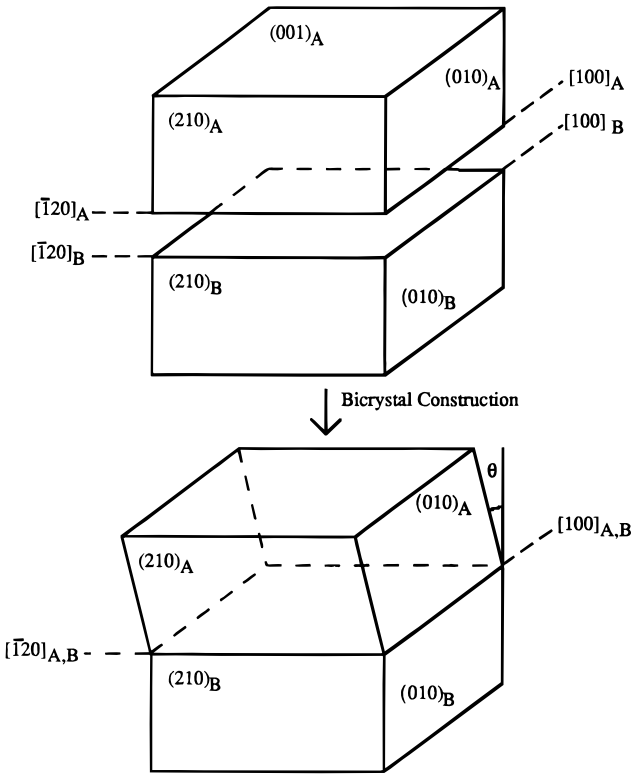

Figure 5. Schematic demonstrating that the (2 1 0) edge (the [1̄ 2 0] direction) on the (0 0 1) cross section is taken as a reference for the rotation axis during the construction of the tilt bicrystals.

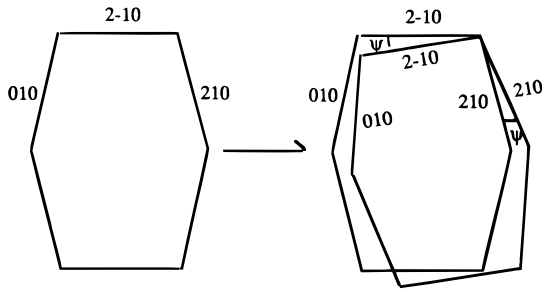

Figure 6. Schematic of the construction of a pure twist bicrystal. We take one edge, e.g., the (2 1 0) edge, on one cut surface as the reference, and rotate the corresponding edge on another surface about the [0 0 1] axis under optical microscope by an angle of ψ; a monomer twist bicrystal with ψ degree twist is then defined and constructed.

Sectioning a DCHD diacetylene monomer single crystal perpendicular to the [0 0 1] direction is experimentally challenging due to the brittle nature of the organic crystals. The mechanical damage introduced in sectioning can easily destroy the whole crystal. We therefore developed a solvent-cutting technique to minimize mechanical damage, similar to that used to section organic photoconductor samples.[56] Figure 7 is a schematic of the solvent-cutting saw used to section DCHD diacetylene single crystals. A DCHD monomer single crystal is mounted on a sample stage with the [0 0 1] direction perpendicular to the stainless steel cutting wire. The wire passes through an acetone solvent bath before it touches the crystal and carries acetone onto the crystal. The acetone dissolves DCHD at the cut and minimizes mechanical damage. By using this technique, we have successfully sectioned DCHD diacetylene monomer crystals with cross sectional sizes up to 20 mm^2 by using a South Bay Technologies Inc. Model 850 wire saw. Panels a and b of Figure 8 show respectively

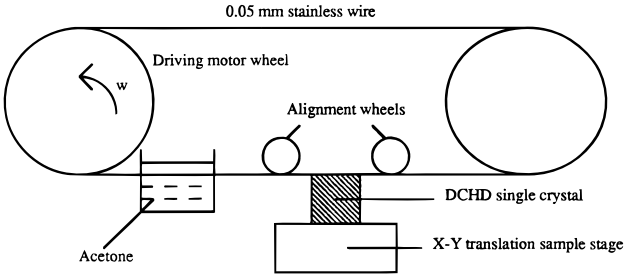

Figure 7. Schematic of the solvent-cutting saw (South Bay Technologies Inc., Model 850) used to section DCHD diacetylene single crystals. A DCHD monomer single crystal is mounted on sample stage with the [0 0 1] direction perpendicular to the stainless steel cutting wire. The wire passes through an acetone solvent bath before it touches the crystal. The acetone helps to dissolve the DCHD at the cut and minimizes mechanical damage.

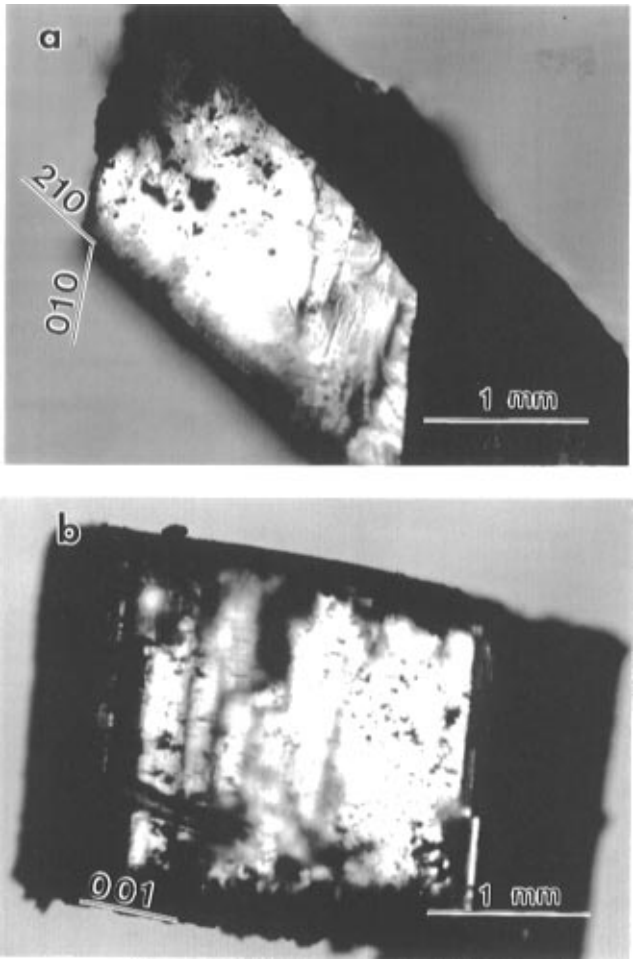

Figure 8. Optical micrographs showing (a) the top and (b) side views of a DCHD diacetylene monomer single crystal seed sectioned with the solvent-cutting saw in Figure 7.

the top and side views of a DCHD monomer single crystal seed cut with this method. In order to successfully section the brittle DCHD diacetylene monomer crystals, high-quality single crystals need to be chosen. As discussed in more detail elsewhere,[57] crystal transparency to visible light in an optical microscope can be used to measure the quality of DCHD diacetylene monomer single crystals. Crystals with a higher density of defects scatter more light and are easily cracked during the process of sectioning.

To construct a DCHD diacetylene monomer bicrystal, we need to put two seed crystals together with a defined

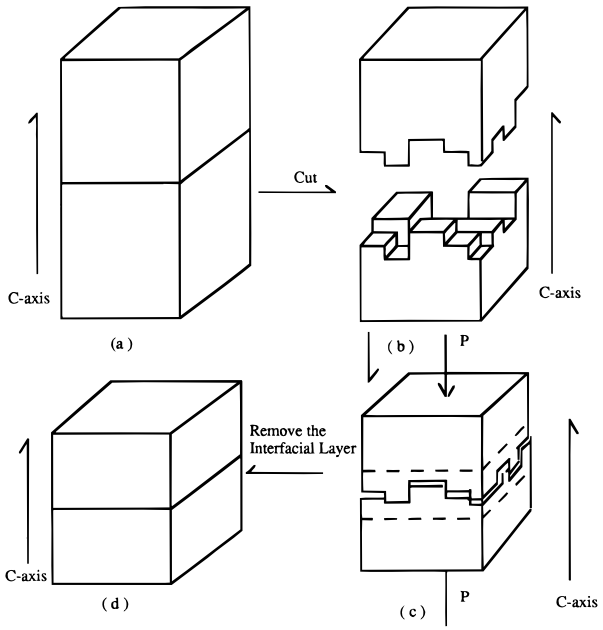

Figure 9. Schematic of the procedure for solution growth of DCHD diacetylene monomer bicrystals. We first saturate acetone with DCHD monomer. We then add an amount of acetone into solution capable of dissolving $^1/_4$–$^1/_5$ of the original seeds to make a slightly desaturated solution. We then immerse the whole assembly of the constrained seed crystals into this desaturated solution and seal it by sculpture modeling compounds. After removing an interfacial layer of material and having the solution reach the saturated point again, we grow diacetylene monomer bicrystals by slow evaporation of solvent.

twist or tilt grain boundary and hold them firmly to avoid shaking or shifting, which might change the boundary geometry. During the construction of a pure twist monomer bicrystal, we utilize the characteristic shape of the (0 0 1) cross section as described earlier. A DCHD diacetylene single crystal is sectioned perpendicular to the [0 0 1] direction, making (0 0 1) the grain boundary plane. We take one of the edges on the (0 0 1) cross section such as the (2 1 0) as a reference and rotate it by ψ degrees during observation with an optical microscope. To avoid shaking or shifting, which might change the boundary geometry, we apply a slight pressure of 0.1−0.2 MPa along the [0 0 1] direction with a Mitutoyo No. 7056 dial gauge and immerse the whole set in DCHD solution to grow a twist monomer bicrystal.

The procedure for constructing a tilt bicrystal is slightly different. Before joining the two seed crystals together, the cut surfaces need to be polished to define the tilt angle. As shown in Figure 4a, one cut surface is polished further after solvent-aided sectioning to construct an asymmetric tilt grain boundary with a tilt angle θ. A glass sliding channel is designed to hold the seed crystals together by gravity when one seed slides on top of the other. The whole set is immersed in a solvent less dense than DCHD itself so that the DCHD seed crystals can be held together.

Even though the seed crystals are held closely together, they are not necessarily in contact at a microscopic level. This initial surface roughness prevents intimate contact and resists bonding during the process of bicrystal formation. We thus dissolve material at the boundary to ensure contact at the interface, as shown in Figure 9. The detailed procedure is as follows. We first saturate acetone with DCHD monomer. We then add an amount of acetone into solution capable of dissolving $^1/_4$–$^1/_5$ of the original seeds to make a slightly

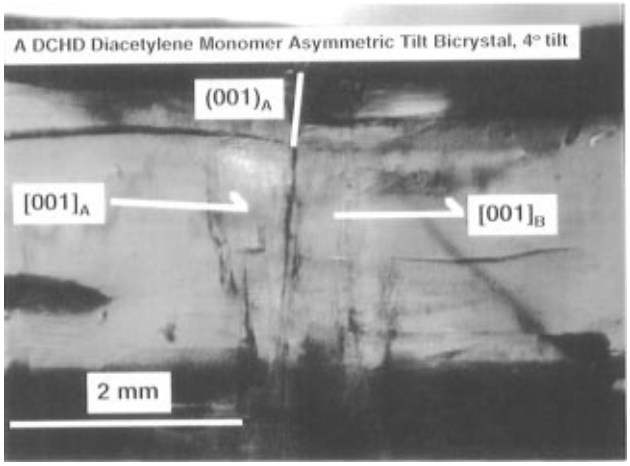

Figure 10. Polarized optical micrograph showing a DCHD diacetylene monomer asymmetric tilt bicrystal with 4° of tilt of the [0 0 1] about the [1 2 0] axis constructed by the routines described in Figures 4 and 9. The grain boundary plane is the (0 0 1) of the left grain and the plane that makes 4° with (0 0 1) of the right grain.

desaturated solution. We immerse the constrained seed crystals with defined boundary geometry into this desaturated solution and seal it by sculptural modeling compounds. After removing an interfacial layer of material and having the solution reach the saturated point again, we grow the diacetylene monomer bicrystals by slow evaporation of solvent.

Figure 10 is a polarized optical micrograph showing a DCHD diacetylene monomer asymmetric tilt bicrystal constructed in our laboratory. The [0 0 1] direction is tilted by 4° about the [$\bar{1}$ 2 0] axis and the (2 1 0) edges are kept parallel to one another during the construction. The grain boundary plane is the (0 0 1) for the left grain and the plane, which makes a 4° angle with the (0 0 1) plane for the right grain.

BICRYSTAL POLYMERIZATION

Diacetylenes can be polymerized either thermally or by irradiation. DCHD diacetylene can be polymerized completely by using Co γ-irradiation with a total dose of 80 Mrad or by thermal polymerization at 150 °C for 72 h.[32] We have used both thermal and irradiation polymerization to transform DCHD diacetylene monomer bicrystals into polymer bicrystals. Figure 11 is an optical micrograph showing a DCHD diacetylene polymer asymmetric tilt bicrystal having a 4° of tilt of the [0 0 1] about the [$\bar{1}$ 2 0] axis, obtained by thermally transforming the monomer bicrystal precursor at 150 °C for 72 h.

The transformation of DCHD diacetylene monomer bicrystals into polymer bicrystals was found to be dependent on two major factors: grain boundary geometry and polymerization method. Table 1 shows a list of bicrystals we have constructed and summarizes the conditions for success in transforming DCHD diacetylene monomer bicrystals into polymer bicrystals.

As revealed in Table 1, the amount of misorientation, either tilt or twist, is critical for the transformation. Basically, we found that small-angle grain boundaries remain intact and large-angle grain boundaries break during the transformation. Tilt bicrystals with tilting angles θ larger than 15° and twist bicrystals with twisting angle ψ larger than 20° all debonded at the grain boundaries during the transformation. To successfully transform the DCHD diacetylene monomer

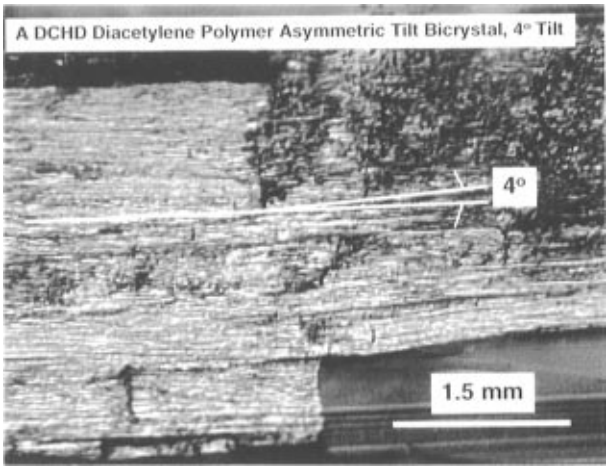

Figure 11. Optical micrograph showing a DCHD diacetylene polymer asymmetric tilt bicrystal having 4° of tilt of the [0 0 1] about the [1 2 0] axis, obtained by thermal polymerization of the monomer bicrystal precursor at 150 °C for 72 h.

Table 1. Summary of DCHD Diacetylene Polymer Bicrystal Construction

type	angle (deg)	results	polymerization
twist	2	good	thermal
twist	5	good	thermal
twist	10	good	thermal
twist	15	good	thermal
twist	20	good	thermal
twist	25	broken	thermal
tilt	4	good	thermal
tilt	8	good	thermal
tilt	15	good	thermal
tilt	20	broken	thermal
twist	5	good	X-ray
twist	5	good	γ-irradiation
twist	10	good	γ-irradiation
twist	15	broken	γ-irradiation
twist	20	broken	γ-irradiation
tilt	0	good	X-ray
tilt	5	good	γ-irradiation
tilt	10	broken	γ-irradiation
tilt	15	broken	γ-irradiation
tilt	45	broken	γ-irradiation

bicrystals into polymer bicrystals, the amount of misorientation must be kept small. This observation has the important implication that the polymer chain continuity through grain boundaries is a decreasing function of the misorientation angles between the grains. It is also consistent with Day and Lando's suggestion that large-angle grain boundaries between crystal domains do not facilitate polymerization.[18]

We have found from our studies that the geometrical conditions for bicrystal polymerization depend on the polymerization methods used in the transformation. As shown in Table 1, the grain boundary geometrical condition is more restricted if we use radiation-induced polymerization to transform the monomer bicrystals. Bicrystals with tilting angles larger than 10° or twisting larger than 15° all debonded at grain boundaries during radiation polymerization with γ-rays, electrons, and X-rays. However, bicrystals thermally transformed can allow misorientations up to 20° in tilt and 25° in twist.

The results shown in Table 1 raise questions about the transformation mechanism at the grain boundaries as the monomer bicrystals proceed *via* a solid-state transformation to polymer bicrystals. To provide further information about this subject, we need to develop techniques to observe the polymerization at the molecular level. TEM provides the high resolution required for this study. But, as for other organic solids, diacetylene monomer and polymer crystals are very sensitive to the electron beam. Electron beam damage has been an obstacle to the application of TEM in microstructural studies of organic polymer solids. We have successfully developed techniques to minimize electron beam damage in TEM by controlling the dose rate. This has enabled us to dynamically image the DCHD diacetylene monomer−polymer solid-state phase transformation.[13] White Beam synchrotron X-ray topography (WBSXT) has been another high-resolution tool in microstructural studies. The exposure time can be shortened significantly to minimize the X-ray radiation damage to organic materials. It also provides the ability to observe the dynamic, microstructural evolution in bulk samples. WBSXT can be used to characterize the diacetylene polymerization and microstructure of the bicrystals.[11,57] Here we show how WBSXT of DCHD monomer bicrystals can provide an estimate of the accuracy of the monomer bicrystal construction.

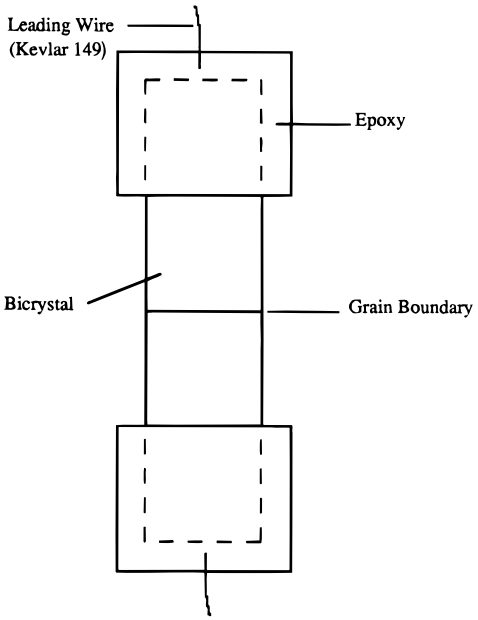

Figure 12. Schematic showing the apparatus for mechanical strength testing. DCHD diacetylene bicrystals are embedded in epoxy. Two yarns of Kevlar fibers are coaxial with the bicrystal samples, lead out of the epoxy, and are grasped by the mechanical arms of the Instron machine.

EXPERIMENTAL SECTION

1. Mechanical Testing. Figure 12 schematically shows the apparatus for mechanical strength testing. DCHD diacetylene bicrystals are embedded in epoxy. Two Kevlar 149 threads are used to provide a mechanical connection to an Instron 4204 testing frame with fiber grips. The mechanical strength and modulus of the Kevlar 149 and epoxy were both tested before the experiment for calibration of the machine compliance according to ASTM D3379. The cross-head speed was 1 mm/min. The crystal dimensions were measured by an optical microscope attached to a Quadra 700 with the image processing software NIH Image.

2. Transient Photoconductivity. (i) Sample Preparation. DCHD diacetylene polymer bicrystal samples for transient photoconductivity measurements are prepared in an Auston gap transmission geometry. Silver thin films are deposited on each side of a grain boundary by vacuum evaporation. Figure 13a is an optical micrograph showing a 80 μm Auston gap across a 4° asymmetric tilt grain boundary. The Auston gap sizes can be reproducibly manipulated down

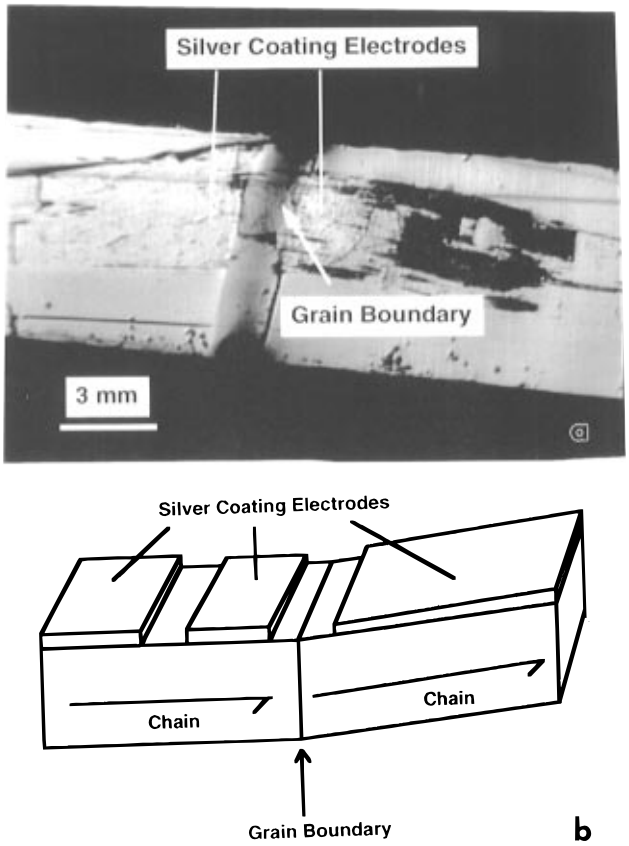

Figure 13. (a) Optical micrograph showing a 80 μm Auston gap across a 4° asymmetric tilt grain boundary. The Auston gap sizes can be manipulated down to the order of 10 μm. (b) Schematic showing an Auston gap containing a grain boundary in the middle and an Auston gap on the surface of a single crystal region as a reference.

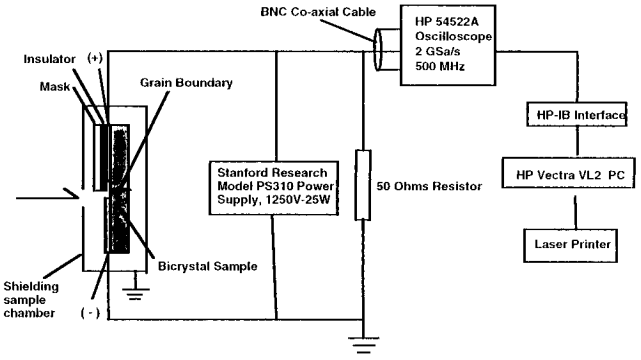

Figure 14. Schematic of the experimental setup to measure transient photoconductivity. A diacetylene polymer bicrystal sample is placed in an Auston transmission line with the grain boundary in the middle of the gap and masked by a metallic thin foil. Charge carriers are generated by a pulsed UV nitrogen laser (Laser Photonics, LN1000). An electrical field is applied across the grain boundary by a voltage supply (Stanford Research System, PS310) driving the carriers through the grain boundary. The transient voltage drop across a 50 Ω resistor is detected by a 500 Hz Hewlett-Packard 54522A oscilloscope with sampling rate of 2 GSa/s. The photoconductivity data are analyzed with an HP-IB interface to a Hewlett-Packard Vectra VL2 computer.

to 10 μm. An aluminum foil mask is located on top of the grain boundary, as shown in Figure 14, to protect the grain boundary from direct laser illumination. This only allows laser photons to bombard the sample at the gap between the mask and uncovered silver electrode.

(ii) Transient Photoconductivity Measurements. Figure 14 is a schematic of the transient photoconductivity testing system. A diacetylene polymer bicrystal sample is placed in an Auston transmission line with the grain boundary in the middle of the gap and masked by a metallic thin foil. Charge carriers are generated by a pulsed (600 ps) UV nitrogen laser (Laser Photonics, LN1000) within a skin depth which is uncovered by the mask. The UV laser has a wavelength of 337 nm, which corresponds to a photon energy of 3.67 eV, sufficient to overcome the band gap of the DCHD polydiacetylene (2.4 eV)[30] and generate charge carriers. An electric field (Stanford Research System PS310 1250 V-25 W) drives the carriers through the grain boundary. A transient photocurrent passes through the transmission line, and the voltage drop across a 50 Ω resistor is detected by a 500 Hz HP 54522A oscilloscope with sampling rate of 2 GSa/s. The characteristic carrier relaxation time in diacetylene polymer single crystals is on the order of 1−10 ns for the gap sizes used in our experiments. Using the HP 54522A oscilloscope we are able to precisely record the photocurrent wave forms and examine the carrier drift as a function of grain boundary geometry under different electrical field strengths. The photoconductivity data are finally analyzed by using an HP-IB interface to a Hewlett-Packard Vectra VL2 computer. In order to isolate the effect of the grain boundary itself, we make at least one Auston gap across a single-crystal region in the same bicrystal sample as a reference, as shown in Figure 13b. We then compare the properties of a grain boundary to its single crystal.

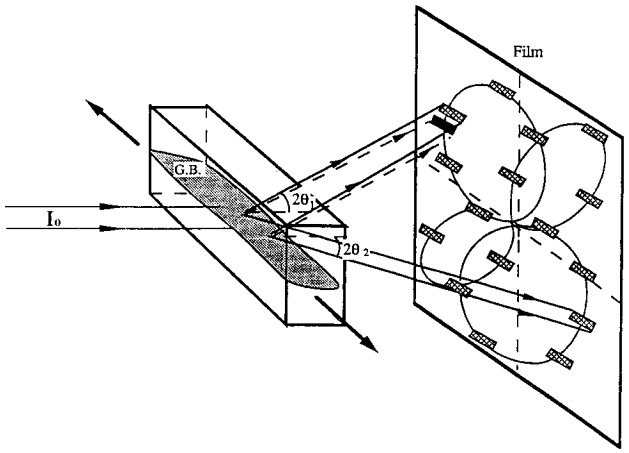

Figure 15. Schematic of the WBSXT transmission Laue method. The sample here is a bicrystal with a small-angle grain boundary. The Laue pattern consists of two single patterns from each component grain superimposed on one another. The misorientation causes the topographic image to split, giving rise to a grain boundary image shift. Figure provided by Z. Zeng.

3. Microstructure. The microstructure of the DCHD monomer and polymer bicrystals was studied with optical microscopy (Leitz Ortholux II), low-voltage scanning electron microscopy (Hitachi S800 LVSEM), environmental scanning electron microscopy (ElectroScan ESEM), transmission electron microscopy (120 kV Philips 420 TEM, 200 kV JEOL 2000 FX STEM, and 400 kV JEOL 4000 EX HREM), and atomic force microscopy (Digital Instruments Nanoscope III AFM with multimode attachment).

To determine the accuracy of the construction of the diacetylene monomer bicrystals, we also developed methods to characterize the grain boundary geometry by WBSXT. WBSXT was used previously in the microstructural characterization of diacetylene single crystals.[11] Due to the high flux and collimation of the synchrotron X-ray source, we found that the exposure time required to record WBSXT diffraction patterns or topographs can be shortened significantly and the samples can be observed in the bulk.

Figure 15 shows a schematic of a WBSXT Laue transmission experiment on a bicrystal.[58] If misorientation exists between the grains, a single topograph will break up into two split grain boundary images, and the diffraction pattern would consist of two subpatterns attributed to each grain. The amount of misorientation between the crystals can be calculated by measuring the amount of grain boundary image separation.

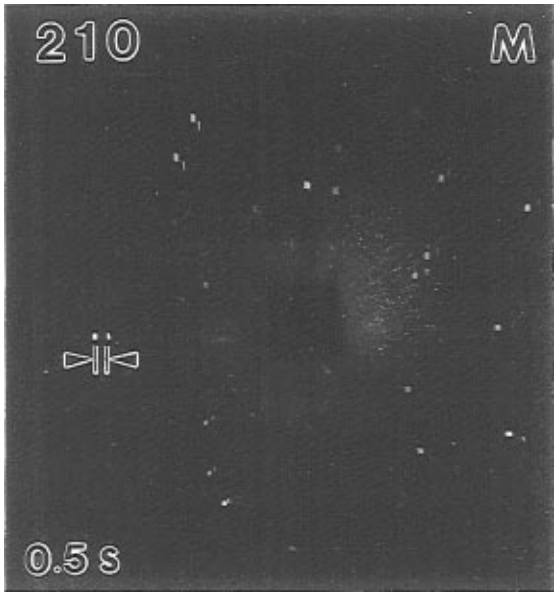

Figure 16. WBSXT diffraction pattern from a DCHD diacetylene monomer bicrystal designed to have no tilt between the grains. The topographic pattern is split into two, indicating there is a slight misorientation which develops during the construction of the monomer bicrystal. By measuring the amount of image separation, the misorientation was calculated to be 0.6°.

In order to test the accuracy of our construction methodology, we created a bicrystal in which we attempted to rejoin the crystals so there was no net misorientation across the interface. Figure 16 is a composite WBSXT transmission Laue diffraction pattern of such a bicrystal. The topographic diffraction pattern is split into two, indicating there is a slight misorientation developed during the construction of the monomer bicrystal. By measuring the image separation, the misorientation is calculated to be 0.6°. There is no vertical image shift on the WBSXT diffraction pattern in Figure 16. Hence, the [0 0 1] direction is tilted by 0.6° about the [$\bar{1}$ 2 0] axis. The misorientation during the construction of DCHD diacetylene monomer bicrystals can therefore be controlled to within 1°.

RESULTS AND DISCUSSION

In terms of the geometrical classification scheme that has been presented for grain boundaries in extended-chain polymers,[19] the tilt boundaries we have constructed are ACR boundaries, while the twist boundaries are ACI boundaries. Since both of these grain boundaries disrupt the covalent bond connectivity, they are expected to have the highest energy and hence the most dramatic impact on macroscopic properties.

Depending on the degree of tilt and twist, grain boundaries can also be classified into (a) small (or low) angle and (b) large (or high) angle grain boundaries. Small-angle grain boundaries are usually described by arrays of discrete lattice dislocations. At a small-angle-tilt grain boundary, two crystals meet at an angle θ by forming a series of edge dislocations of Burgers vector b a distance D apart along the grain boundary plane, where b, D, and θ are related by the equation $D = b/\theta$.[59] At a small-angle twist grain boundary, it is usual to see local structural relaxations which lead to the formation of a network of distributed screw dislocations. Large-angle grain boundaries occur in which θ or $\psi > 30°$ and the dislocation model breaks down.[54] Wilson and Martin directly imaged a small-angle-tilt grain boundary in DCHD diacetylene polymer droplets and found that the boundary structure was formed by the association of edge dislocations.[60]

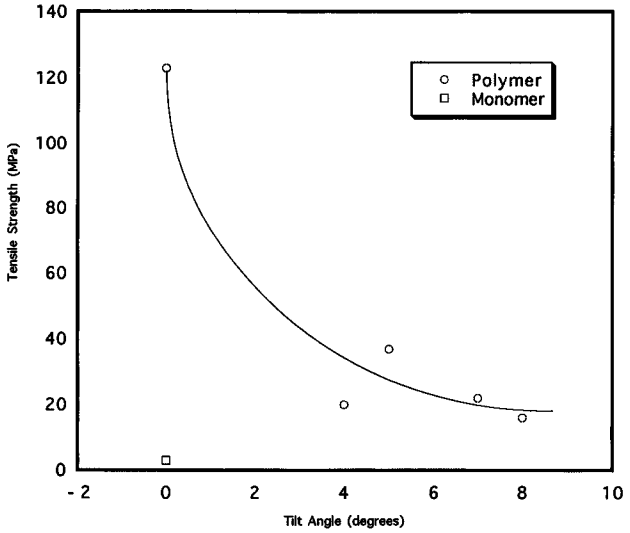

Figure 17. Plot showing the mechanical strength of tested DCHD diacetylene polymer bicrystals with asymmetric tilt grain boundaries as a function of tilt angle. The mechanical strength decreases systematically with increasing tilt angle. After introducing a few degrees of misorientation by tilting the polymer chains, the mechanical strength of the polymer bicrystals is still significantly higher than that of the monomer single crystals.

(i) Mechanical Strength. Due to the conjugated, extended backbone of the polymer chains, diacetylene polymer crystals have high mechanical strength in the polymer chain direction. By measuring the mechanical strength of the bicrystals as a function of misorientation, it should be possible to explore the ability of the chains to continue through the grain boundary. In particular, if the strengths of the bicrystals are higher than that of the monomer crystal, this would provide evidence that a certain number of chains are continuous through the interface.

Figure 17 summarizes the mechanical strengths of tested DCHD diacetylene polymer bicrystals with asymmetric tilt grain boundaries. The mechanical strength of the bicrystals decreases dramatically as a function of increasing tilting angle. Furthermore, at low angles the mechanical strengths of the polymer bicrystals are still significantly higher than those of the monomer single crystals. From Figure 17, one can see that tilting the polymer chains by 4° reduces the mechanical strength from 124 MPa for polymer single crystals to 35 MPa for the polymer bicrystal. While this is a considerable loss in strength from a small amount of misorientation, it is still much higher than that of the monomer single crystals (2 MPa).

These results indicate that small-angle-tilt grain boundary defects play an important role in determining the mechanical properties of DCHD diacetylene polymers. Our data also suggest that a certain number of covalent, conjugated polymer chains do continue through the grain boundary. The chain continuity is correlated to the amount of mechanical strength loss associated with the grain boundaries. If we make the assumption that the ultimate strength is directly related to the number of covalent bonds formed across the interface, then our results indicate that with a 4° tilt at the grain boundary, only 30% of polymer chains are so connected.

As the tested DCHD diacetylene polymer bicrystals reached their mechanical strength, all of the samples broke at the grain boundaries. Using an environmental scanning electron microscope (ESEM), we observed the

Figure 18. (a) ESEM micrograph showing the fracture surface of a bicrystal sample with an asymmetric 8° twist grain boundary. (b) Fracture surface of DCHD monomer single crystal.

fracture surfaces. The fracture surface of the monomer bicrystal (Figure 18a) is fairly flat (less than 1 μm height fluctuations), with cracks evident in certain characteristic crystallographic directions. However, the bicrystal surface (Figure 18b) shows significantly more surface roughess, with large features (50−100 μm) reminiscent of the fibrillar fracture morphology seen in the failure of the polymer crystals. There were regions on the fracture surface of the bicrystal where there was considerably more extensive deformation than on others, suggesting a certain degree of heterogeneity of reaction efficiency at different positions on the grain boundary.

(ii) Transient Photoconductivity. Figure 19 shows the maximum transient voltage drop across a 50 Ω resistor as a function of the grain boundary geometry. There is a significant decrease in photocurrent intensity with increasing tilting angle of the DCHD diacetylene polymer bicrystals. The small-angle-tilt grain boundary defects evidently dissipate carriers drifting along the molecular backbone.

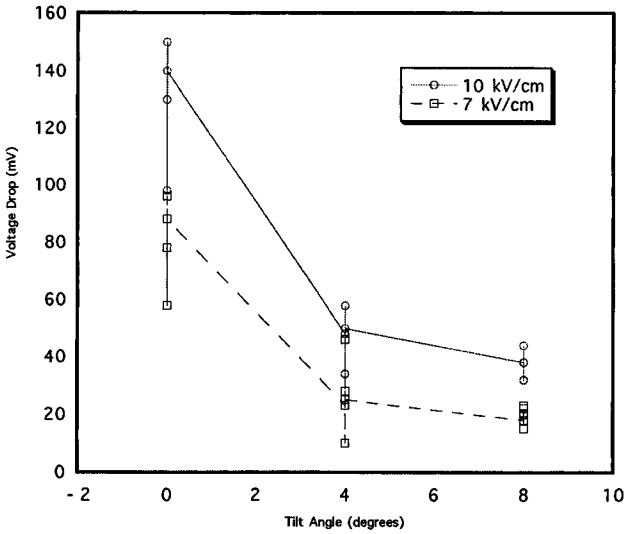

Figure 19. Maximum transient voltage drop across a 50 Ω resistor as a function of the DCHD grain boundary geometry. There is a significant reduction in the bicrystal photocurrent intensity with increasing tilt angle. The data are shown for two applied fields: 10 and 7 kV/cm.

It is expected that a small-angle asymmetric tilt grain boundary, which does not allow for all of the chains to remain connected across the interface, will be composed of a number of misfit edge dislocations and chain ends. The edge dislocations should have [*hk*0] type Burger's vectors perpendicular to the [0 0 1] polymer chain direction. These chain ends and edge dislocations would interrupt the polymer chain continuity at the grain boundary and perturb carrier drift. Small-angle-tilt grain boundaries might act as carrier sinks to charges traveling along the molecule, reducing the photocurrent intensity.

If each chain connected across the grain boundary provides a pathway for the photocurrent, it is possible to relate the photocurrent intensity to grain boundary geometry. I represents the photocurrent intensity through a small-angle-tilt grain boundary and is related to the photocurrent intensity of the perfect single crystal I_0 by $I = fI_0$, where f represents the fraction of the polymer chains or semiconductive wires passing through the grain boundaries. Increasing the misorientation θ means more misfit edge dislocations are needed to accommodate the deformation in the vicinity of the grain boundaries. This would create more carrier traps at the grain boundaries and reduce the number of the polymer chains or semiconductive wires continuing through the grain boundaries.

The experimentally observed reduction of photocurrent intensity caused by the small-angle-tilt grain boundaries (Figure 19) suggests that the extra chain ends and edge dislocations at the interface interrupt charge carrier drift. The O-lattice theory describes grain boundary geometry by relating lattice points of one component crystal to another as a function of the misorientation.[61] By considering the fact that misfit dislocations exist at grain boundaries, Bollman extended the geometrical description of the O-lattice to include relaxations. In his theory, the O-lattice sites are

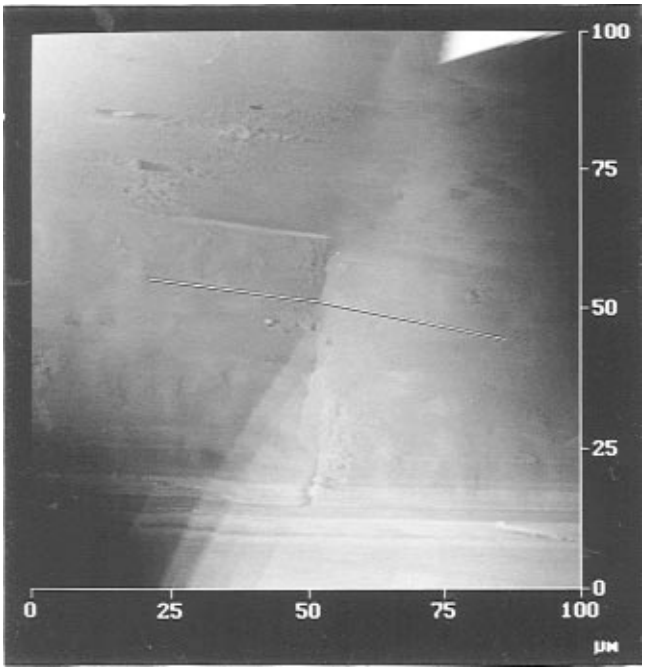

Figure 20. AFM micrograph showing the morphology of an asymmetric 4° tilt grain boundary of a DCHD diacetylene polymer bicrystal. The field of view is 100 μm by 100 μm.

considered as nucleation sites for relaxation to a more perfect structure with lower grain boundary energy. Similar ideas have been applied to diacetylene bicrystal systems.[62,63] It seems reasonable to assume that relaxed regions surrounding O-lattice sites would allow polymerization while the unrelaxed regions would not. Therefore, the fraction of the relaxed area corresponds to the fraction of covalent polymer chains through the grain boundaries. The rate at which macroscopic properties decrease with misorientation angle is a measure of the local relaxations near the dislocation core. Both the mechanical strength and photoconductivity decrease dramatically with increasing misorientation across the boundary.

(iii) Grain Boundary Morphology. By solid-state phase transformation, we can convert the monomer bicrystals into polymer bicrystals as shown by the optical micrograph in Figure 11. However, due to the resolution limitation of optical microscopy, it is difficult to observe the morphology near the grain boundary itself. Also, the surfaces of the seed crystals are not necessarily in full contact at microscopic level after we bring them together to construct the grain boundary.

Figure 20 is an 100 $\times$ 100 μm^2 AFM micrograph showing an asymmetric 4° tilt grain boundary. The direction of the chain axis on either side of the interface is indicated. The two component seed crystals are in microscopic contact without any significant discontinuities, reorganization, or voids at the grain boundary. Figure 21 is a ESEM image providing a 3-D view of a DCHD diacetylene polymer bicrystal with a 15° asymmetric tilt grain boundary.

A transmission electron micrograph of the grain boundary interface of an engineered DCHD bicrystal is shown in Figure 22. As in the OM, SEM, and AFM images, there is no evidence for any large voids or any dramatic reorganization of material near the grain boundary. At the interface, there are regions where there seems to be good contact between the crystals, whereas in other regions the interactions are not as well established. The data are consistent with a model in

Figure 21. ESEM micrograph showing the morphology of an asymmetric 15° tilt grain boundary in DCHD.

which there are discrete domains within which the chains are continuous, and others where the chains are not continuous. This interpretation is also consistent with SEM data showing certain regions with large amounts of fibrillar deformation (as found in the polymer) and other regions with a flatter surface (as found in the monomer). A schematic diagram illustrating this morphology is shown in Figure 23.

High-resolution studies of the dislocation core structure in DCHD have shown that the distortions are highly localized into parabolic regions parallel to the Burger's vector.[63] The rates at which the macroscopic mechanical, and photoconductive properties of the polymer bicrystals decrease with angle (Figures 17 and 19) are generally consistent with these observations.

CONCLUSIONS AND FUTURE WORK

The ability to create polymer bicrystals with precisely controlled geometries requires the synthesis and purification of DCHD diacetylene monomer, controlled crystallization, crystal cutting and joining, polymerization, and finally mechanical and photoconductive testing. To date, we have constructed and characterized more than 40 DCHD polydiacetylene bicrystal samples with well-defined grain boundary defect geometries.

The photoconductivity data (Figure 19) were obtained from 14 different samples: four single-crystal reference samples, five samples with 4° of tilt, and five samples with 8° of tilt. The mechanical testing data were obtained from five different bicrystal samples with various amounts of tilt as indicated in Figure 17.

Because of the considerable experimental effort required to create the polymer bicrystal samples in a reliable and consistent manner, our available statistics are limited. Nevertheless, our results clearly indicate that both the mechanical strength and electronic transport properties of crystalline polymers are significantly decreased by the presence of grain boundary defects which interrupt the connectivity of covalent bonds.

We believe it is now necessary to devote additional effort in constructing and characterizing bicrystals with smaller systematic variations in tilt and twist near zero angle (i.e., to make small-angle grain boundaries with misorientations less than 5°). By examining the rate at which the macroscopic properties of the bicrystals decrease with increasing tilt angle in this regime, it should be possible to obtain additional information about the nature of the structural reorganization at the

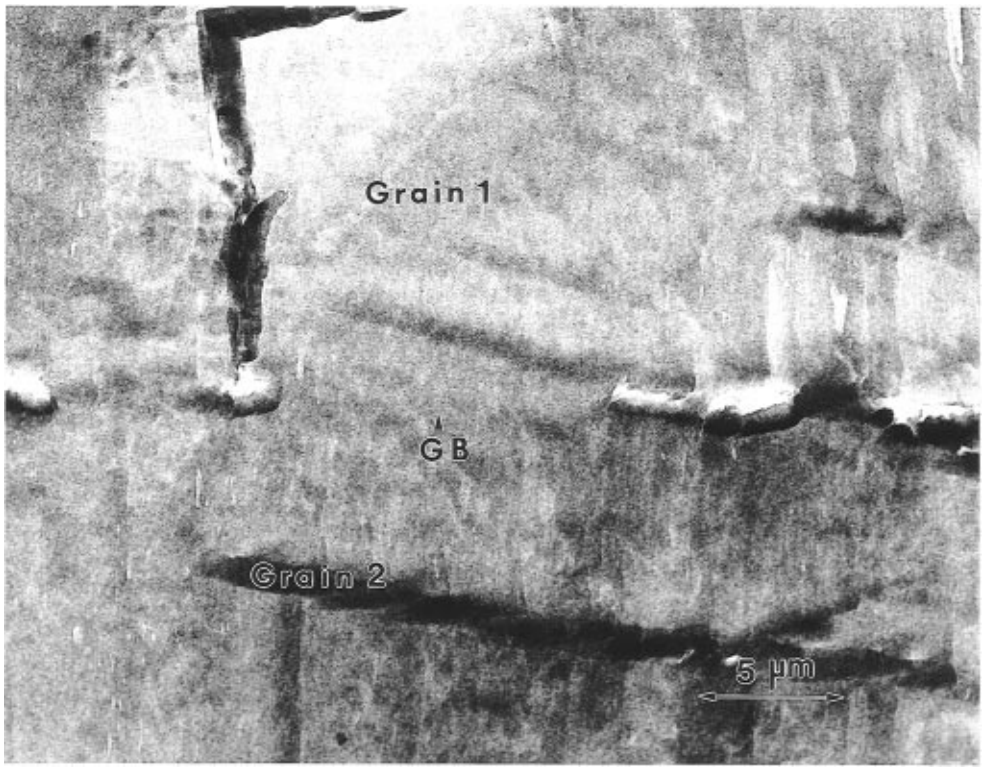

Figure 22. TEM micrograph of a engineered grain boundary in a DCHD polymer bicrystal. The interface (GB) runs from left to right in the center of the micrograph and shows evidence for regions where the chain connectivity is maintained (center) and other regions where it is not (right).

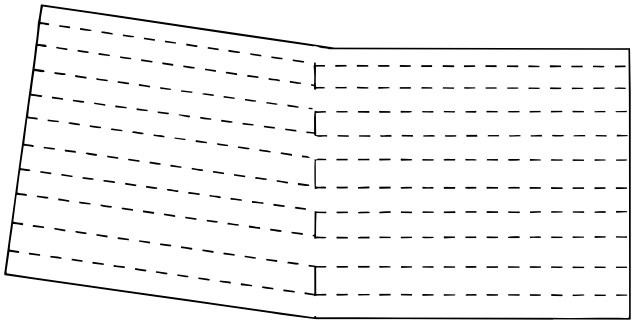

Figure 23. Schematic diagram of the morphology of an asymmetric tilt bicrystal in DCHD.

interface. By constructing and characterizing individual grain boundary defects, it is possible to reveal fundamentally interesting insights about the relationship between the local microstructure of conjugated polymers and their macroscopic mechanical and optoelectronic properties.

In summary, we have shown that DCHD diacetylene polymer bicrystals can be obtained by polymerizing precursor monomer bicrystals in the solid state with controlled grain boundary geometry. The basic procedures include the following: (1) growth of DCHD diacetylene monomer single crystals; (2) solvent-cutting of the single crystals into seed crystals; (3) control of the grain boundary geometry under an optical microscope; (4) regrowth of the monomer bicrystals in solution by slow evaporation of DCHD in organic solvent; and (5) transformation of the DCHD diacetylene monomer bicrystals into polymer bicrystals in the solid state. The relative orientation between component grains can be controlled to within 1° during the construction of DCHD monomer bicrystals.

We have observed that the mechanical strength and transient photoconductivity of polymer bicrystals are both sensitive to a small amount of misorientation of the DCHD diacetylene polymer chains. Both properties decrease with increasing misorientation between the component grains in DCHD diacetylene polymer bicrystals. The mechanical strength testing and transient photoconductive measurements have proven to be useful tools for detecting the polymer chain continuity through grain boundaries.

The analysis of grain boundary morphology in terms of a dislocation model provides the insight that the rate at which the macroscopic properties decrease with misorientation angle is related to the nature and extent of relaxations near the dislocation core. Examinations of the grain boundary morphology by TEM and fracture surface by SEM indicate that there are discrete regions at the interface where the chains are well connected, and other regions where they are not.

More experiments to examine the detailed changes in microstructure, crack propagation, and morphology at the interface are warranted, particularly at small-angles where the interfaces are composed of specific dislocations. It would be possible to probe the influence of dislocations with specific Burger's vectors by tilting the crystals about different zone axes. Such studies would be particularly interesting in polymer systems with highly anisotropic lateral shapes (i.e., in which the *a* dimension was significantly different from *b*).

Future experiments could also focus more attention on the micromechanisms of stress transfer across the interface as a function of misorientation. These studies could include efforts to measure the local strain distribution near the grain boundary by Raman spectroscopy. Finally, we are investigating schemes to exploit the rational construction of specific structural defects for novel optoelectronic polymer-based devices, as has been done for inorganic semiconductors.[64]

Acknowledgment. We extend thanks to Prof. Jeffrey S. Moore and Larry Markoski for helping us in the synthesis of the DCHD diacetylene monomer, to Prof. John Bilello and Dr. Zofia Rek for providing synchrotron X-ray beam time at Stanford Synchrotron Radiation Laboratory, to Ms. Zhen Zeng for her help in the synchrotron X-ray experiments and discussions of white beam synchrotron X-ray topography data, and to Mr. Dan Holbrook for his help in growth of DCHD diacetylene monomer single crystals. This research was sponsored by NSF Grant DMR-9024876, a NSF National Young Investigator Award, and the Michigan Memorial Phoenix project.

References and Notes

(1) Salaneck, W. R.; Bredas, J. L. *Solid State Commun.* **1994**, *92* (1−2), 31.
(2) Dimos, D.; Chandhari, P.; Mannhart, J. *Phy. Rev. B* **1990**, *41*, 4038.
(3) Chandhari, P.; Chi, C. J.; Dimos, D. B.; Mannhart, J. D.; Tsuel, C. C.; U.S. Patent No. 5,162,298, 1992.
(4) Cho, F. Y.; Penunuri, D.; Falkner, R. F., Jr. U.S. Patent No. 5,125,136, 1992.
(5) Wegner, G. *Z. Naturforsch.* **1969**, *24B*, 824.
(6) Baughman, R. H. *J. Polym. Sci.: Polym. Phys. Ed.*, **1974**, *12*, 1511.
(7) Enkelmann, V.; Leyrer, R. J.; Schleier, G.; Wegner, G. *J. Mater. Sci.* **1980**, *15*, 168.
(8) Kaiser, J.; Wegner, G.; Fischer, E. W. *Isr. J. Chem.* **1972**, *10*, 157.
(9) Schultz, J. M. *J. Mater. Sci.* **1977**, *12*, 2258.
(10) Rosemeier, R.; Green, R. E.; Baughmann, R. H. *J. Appl. Phys.* **1981**, *52*, 7129.
(11) Dudley, M.; Sherwood, J. N.; Bloor, D.; Ando, D. J. *J. Mater. Sci. Lett.* **1982**, *1*, 479.
(12) Dudley, M.; Sherwood, J. N.; Ando, D. J.; Bloor, D. *Mol. Crys. Liq. Cryst.* **1983**, *93*, 223.
(13) Liao, J.; Martin, D. C. *Science* **1993**, *260*, 1489.
(14) Young, R. J.; Baughman, R. H. *Polymer* **1978**, *13*, 55.
(15) Young, R. J.; Bloor, D.; Batchelder, D. N.; Hubble, C. L. *Polymer* **1978**, *13*, 62.
(16) Young, R. J.; Dulniak, R.; Batchelder, D. N.; Bloor, D. *J. Polymer. Sci.: Polym. Phys. Ed.* **1979**, *17*, 1325.
(17) Read, R. T.; Young, R. J. *Philos. Mag.* A **1980**, *42* (5), 629.
(18) Day, D.; Lando, J. B. *Macromolecules* **1980**, *13*, 1483.
(19) Martin, D. C.; Thomas, E. L. *Philos. Mag. A* **1991**, *64* (4), 903.
(20) Martin, D. C.; Thomas, E. L. *Macromolecules* **1991**, *24*, 2450.
(21) Gido, S. P.; Thomas, E. L. *Macromolecules*, **1994**, *27*, 6137.
(22) Gido, S. P.; Thomas, E. L. *Macromolecules* **1994**, *27*, 849.
(23) Gido, S. P.; Gunther, J.; Thomas, E. L.; Hoffman, D. *Macromolecules* **1994**, *27*, 6137.
(24) Robinson, I. M.; Yeung, P. H. J.; Galiotis, C.; Young, R. J.; Batchelder, D. N. *J. Mater. Sci.* **1986**, *21*, 3440.
(25) Robinson, I. M.; Galiotis, C.; Batchelder, D. N.; Young, R. J. *J. Mater. Sci.* **1991**, *26*, 2293.
(26) Galiotis, C.; Read, R. T.; Yeung, P. H. J.; Young, R. J. *J. Polym. Sci.: Polym. Phys. Ed.* **1984**, *22*, 1589.
(27) Le Moigne, J.; Kajzar, F.; Thierry, A. *Macromolecules* **1991**, *24*, 2622.
(28) Kajzar, F.; Messier, J. *Nonlinear Optical Properties of Organic Molecules and Crystals*; Chemla, D. S., Zyss, J. Eds.; Academic: New York, 1987; p 51.
(29) Sinclair, M.; McBranch, D.; Moses, D.; Heeger, A. J. *Appl. Phys. Lett.* **1988**, *53*, 2374.
(30) Le Moigne, J.; Thierry, A.; Chollet, P. A.; Kajzar, F.; Messier, J. *J. Chem. Phys.* **1988**, *88*, 6647.
(31) Thakur, M.; Krol, D. M. *Appl. Phys. Lett.* **1990**, *56*, 1213.
(32) Yee, K. C.; Chance, R. R. *J. Polym. Sci.: Polym. Phys. Ed.* **1978**, *16*, 431.
(33) Apgar P. A.; Yee, K. C. *Acta Crystallogr.* **1978**, *B34*, 957.
(34) Enkelmann, V.; Schleier, G.; Wegner, G.; Eichele, H.; Schwoerer, M. *Chem. Phys. Lett.* **1977**, *52*, 314.
(35) Galiotis, C.; Read, R. T.; Yeung, P. H. J.; Young, R. J. *J. Polym. Sci.: Polym. Phys. Ed.* **1984**, *22*, 1589.
(36) Adam, D.; Closs, F.; Frey, T.; Funhoff, D.; Haarer, D.; Ringsdorf, H.; Schuhmacher, P. l; Siemensmeyer, K. *Phys. Rev. Lett.* **1993**, *70*, 457.
(37) Galiotis, C.; Young, R. J.; Yeung, P. H. J.; Batchelder, D. N. *J. Mater. Sci.* **1984**, *19*, 3640.
(38) Baughman, R. H.; Gleiter, X. X.; Sendfield, X. X. *J. Polym. Sci.: Polym. Phys. Ed.* **1975**, *13*, 1871.
(39) Young, R. J.; Bloor, D.; Batchelder, D. N.; Hubble, C. L. *Polymer* **1978**, *13*, 62.
(40) Young, R. J.; Dulniak, R.; Batchelder, D. N.; Bloor, D. *J. Polym. Sci.: Polym. Phys. Ed.* **1979**, *17*, 1325.
(41) Robinson, I. M.; Yeung, P. H. J.; Galiotis, C.; Young, R. J.; Batchelder, D. N. *J. Mater. Sci.* **1986**, *21*, 3440.
(42) Moses, D.; Singer, M.; Heeger, A. J. *Phys. Rev. Lett.* **1987**, *58*, 2710.
(43) Fisher, N. E. *J. Phys.: Condens. Matter* **1992**, *4*, 2533.
(44) Kao, K.-C.; Hwang, W. *Electrical Transport in Solids*; Pergamon Press: New York, 1981.
(45) Donovan, K. J.; Wilson, E. G. *Philos. Mag. B*, **1981**, *44* (1), 9.
(46) Wilson, E. G. *J. Phys. C: Solid State Phys.* **1983**, *16*, 6739.
(47) Donovan, K. J.; Wilson, E. G. *Philos. Mag. B* **1981**, *44* (1), 31.
(48) Donovan, K. J.; Wilson, E. G. *J. Phys. C: Solid State Phys.* **1986**, *19*, L357.
(49) Donovan, K. J.; Freeman, P. D.; Wilson, E. G. In Bloor, D., Chance, R., Eds.; *Polydiacetylenes: Synthesis, Structure and Electronic Properties*; Martinus Nijhoff Publishers: Dordrecht, The Netherlands, 1985.
(50) Kepler, R. G. *Phys. Rev.* **1960**, *119*, 1226.
(51) LeBalance, O. H., Jr. *Chem. Phys.* **1960**, *33*, 626.
(52) Fisher, N. E.; Willock, D. J. *J. Phys.: Condens. Matter* **1992**, *4*, 6613.
(53) Yang., Y.; Lee, J. Y.; Miller, P.; Kumar, J.; Tripathy, S. K. *Solid State Commun.* **1991**, *77*, 763.
(54) Sutton, A. P.; Vitek, V. *Philos. Trans. R. Soc. London A* **1983**, *309*, 1.
(55) Hartshorn, N. H.; Stuart, A. *Practical Optical Crystallogaphy*; Arnold: London, 1964.
(56) Karl, N. *Mol. Cryst. Liq. Cryst.* **1989**, *171*, 157.
(57) Liao, J. Ph.D. Dissertation, The University of Michigan, Ann Arbor, MI, 1995.
(58) Zeng, Z.; Bilello, J. C.; Rek, Z. *Mater. Res. Symp. Proc.* **1993**, *307*, 225.
(59) Read, W. T.; Shockley, W. *Phys. Rev.* **1950**, *78*, 275.
(60) Wilson, P. M.; Martin, D. C. *J. Mater. Res.* **1992**, *7*, 3150.
(61) Bollman, W. *Crystal Defects and Crystalline Interfaces*; Springer-Verlag: Berlin, 1970.
(62) Martin, D. C. Defects in Electro-optically Active Polymer Solids. In *Microgravity Studies of Organic and Polymeric Materials*; Frazier, D. J., Moore, C. E., Cardelino, B. H., Eds.; NASA Conference Publication 3250; NASA Marshall Space Flight Center, Huntsville, AL, 1993.
(63) Wilson, P. M. Ph.D. Dissertation The University of Michgan, Ann Arbor, MI, 1994.
(64) Matare', H. F. *Defect Electronics in Semiconductors*; Wiley Interscience: New York, 1971.

MA950792V